

**Interorbital correlation effects on heavy-electron systems**

Tsuneya Yoshida and Norio Kawakami

*Department of Physics, Kyoto University, Kyoto 606-8502, Japan*

(Received 30 March 2012; published 26 June 2012)

We study an extended periodic Anderson model, which includes correlations between conduction and  $f$  electrons, by employing dynamical mean field theory and continuous-time quantum Monte Carlo simulations. It is clarified how the antiferromagnetic phase, which is stabilized in the ordinary periodic Anderson model, changes into a charge ordered (CO) phase in the strong  $c$ - $f$  interaction region. A systematic analysis of the effects due to the hybridization and the  $c$ - $f$  interaction evidences the existence of a critical end point for the CO transition; the quantum phase transition between the CO phase and the paramagnetic phase is of first (second) order in the weak (moderate) hybridization region. We also address the effects of the Hubbard-type correlations among conduction electrons on the phase diagram.

DOI: [10.1103/PhysRevB.85.235148](https://doi.org/10.1103/PhysRevB.85.235148)

PACS number(s): 75.25.Dk, 75.30.Mb, 75.40.Mg

**I. INTRODUCTION**

Recently, in some heavy fermion systems, the correlation effects between conduction ( $c$ ) electrons and localized ( $f$ ) electrons have led to a surge of interest and various interesting phenomena have been observed. This issue opens a new arena to study heavy fermions beyond standard  $f$ - $f$  correlation effects. A typical example is an unconventional pairing mechanism for superconductivity of  $\text{CeCu}_2(\text{Si}_x\text{Ge}_{1-x})_2$ ,<sup>1</sup> which may not be explained in terms of antiferromagnetic (AF) fluctuations alone.<sup>2-5</sup> In particular, to understand two superconducting domes observed for  $\text{CeCu}_2(\text{Si}_{0.9}\text{Ge}_{0.1})_2$  in the pressure-temperature phase diagram,<sup>4,5</sup> Miyake *et al.* claimed the importance of  $c$ - $f$  electron correlations and proposed that the mechanism of the above unconventional superconductor is related to enhanced valence fluctuations.<sup>6,7</sup> Numerical calculations indeed indicated that  $c$ - $f$  correlations cause a valence transition (VT).<sup>8,9</sup> Another example is a metamagnetic behavior observed in  $\text{YbInCu}_4$ . This compound exhibits the VT with lowering temperature<sup>10,11</sup> and the metamagnetic behavior is observed in  $\text{Yb}_{0.38}\text{In}_{0.62}\text{Cu}_4$ .<sup>12</sup> It was proposed that the VT, which is induced by the interplay of  $c$ - $f$  correlations and magnetic fields, plays an essential role in the metamagnetic behavior in the above compound.<sup>13,14</sup> These facts certainly demonstrate the importance of the  $c$ - $f$  correlation effects, and have spurred intense activities in theoretical studies on this issue.<sup>15-23</sup>

Besides such VTs, the charge ordered (CO) phase highlights another important aspect of the heavy fermions due to strong  $c$ - $f$  correlations. For example, the CO phase is found experimentally in  $\text{Eu}_3\text{S}_4$  at low temperatures. In the CO phase, the valence of rare-earth elements is spatially modulated in the ratio of  $\text{R}^{2+} : \text{R}^{3+} = 2 : 1$ .<sup>24</sup> Some experimental groups proposed that the origin of the CO comes from the strong  $c$ - $f$  interaction.<sup>25</sup> It is interesting to investigate the nature of the CO phase theoretically since it is stabilized in the strong correlation region where several competing interactions are expected to cause intriguing quantum phase transitions. Recently, the instability to a CO phase was discussed theoretically for a square-lattice periodic Anderson model with the fluctuation exchange approximation.<sup>26</sup> It is found that the charge susceptibility at a momentum  $\mathbf{q} = (\pi, \pi)$  is enhanced as the  $f$ -electron

level becomes shallow, suggesting the tendency toward a CO instability. However, characteristic behaviors near the CO phase are not so clear since they employ a weak-coupling approach. For example, the CO phase is considered to be stabilized due to the competition between  $f$ - $f$  correlations and  $c$ - $f$  correlations, but the systematic study is still lacking.

In this connection, it is instructive to mention a phenomenological study on a hidden ordered phase of  $\text{URu}_2\text{Si}_2$ ; it is proposed that the  $c$ - $f$  electron correlation would cause a hybridization-modulated order with an incommensurate wave vector, which could be a possible origin of the hidden ordered phase.<sup>27</sup> In addition, the modulation of effective hybridization could induce the CO as a secondary effect.<sup>28</sup> This also motivates us to investigate the  $c$ - $f$  electron correlations in more detail microscopically.

In this paper we address the  $c$ - $f$  correlation effects in heavy-fermion systems with particular emphasis on how the CO state emerges via the competition between other phases. Our detailed study on the CO phase will be complementary to and much more extensive than the preceding work.<sup>29</sup> We discuss how the AF phase changes into the CO phase in the strong  $c$ - $f$  correlation region by combining dynamical mean field theory (DMFT)<sup>30-32</sup> and continuous time-quantum Monte Carlo (CT-QMC) method, which enables us to study the system with high accuracy.<sup>33-35</sup> We also investigate the correlation effects of conduction electrons on the phase diagram.

This paper is organized as follows. First, the model and the method are briefly explained in the next section. In Sec. III the  $c$ - $f$  correlation effects on heavy fermion systems are discussed. Here it is revealed that the CO transition is of first order in general, but it has a critical end point beyond which the system shows second-order critical properties. We then discuss the effects of Hubbard-type correlations between conduction electrons in Sec. IV, and elucidate that they mainly modify the AF properties, but have little effects on the CO phase. A brief summary is given in the last section.

**II. MODEL AND METHODS**

We study an extended periodic Anderson model including  $c$ - $f$  correlations besides ordinary  $f$ -electron correlations. The

Hamiltonian reads

$$H = H_{\text{PAM}} + U_{cf} \sum_{i\sigma\sigma'} n_{i\sigma}^c n_{i\sigma'}^f + U_{cc} \sum_i n_{i\uparrow}^c n_{i\downarrow}^c,$$

$$H_{\text{PAM}} = -t \sum_{(i,j),\sigma} c_{i\sigma}^\dagger c_{j\sigma} + \epsilon_f \sum_{i,\sigma} n_{i,\sigma}$$

$$+ V \sum_{i,\sigma} (c_{i\sigma}^\dagger f_{i\sigma} + \text{H.c.}) + U_{ff} \sum_i n_{i\uparrow}^f n_{i\downarrow}^f, \quad (1)$$

where  $c_{i,\sigma}$  ( $f_{i,\sigma}$ ) is an annihilation operator of  $c$  ( $f$ ) electron at site  $i$  in spin state  $\sigma = \uparrow, \downarrow$ . The  $c$  electrons are itinerant with the hopping integral  $t$  while  $f$  electrons are localized with the energy  $\epsilon_f$ . The hybridization between  $c$  and  $f$  electrons at the same site is represented by  $V$ . Repulsive interactions between  $f$  electrons ( $c$  and  $f$  electron) are given by  $U_{ff}$  ( $U_{cf}$ ). We will also address the effects of the Hubbard type interaction  $U_{cc}$  between  $c$  electrons in Sec. IV. For simplicity we employ the Bethe lattice with its bandwidth  $2D$ , and consider the half-filled symmetric band by setting  $\mu = \frac{1}{2}(U_{cc} + 2U_{cf})$  and  $\epsilon_f = \frac{1}{2}(U_{cc} - U_{ff})$ , where  $\mu$  is the chemical potential.

We analyze the above model by means of DMFT and CT-QMC simulations. In DMFT, a lattice problem is mapped to an effective impurity problem, and then the impurity Green function ( $G_{\text{imp}\sigma}$ ) is obtained self-consistently.<sup>30-32</sup> These self-consistent equations are simplified for our Bethe-lattice structure; the equations for the paramagnetic (PM) phase are simplified as

$$[g_\sigma^{-1}(i\omega)]_{cc} = i\omega + \mu - \left(\frac{D}{2}\right)^2 [G_{\text{imp}\sigma}(i\omega)]_{cc}, \quad (2)$$

where  $g_{cc\sigma}(i\omega)$  is the effective Green function for  $c$  electrons with spin  $\sigma$ . Long-range ordered phases are treated with a sublattice method, where the order parameter for the AF (CO) phase is defined by  $m_{c(f)} = \frac{1}{2}(n_\uparrow^{c(f)} - n_\downarrow^{c(f)})$  [ $\rho = \frac{1}{2} \sum_\sigma (n_\sigma^c - n_\sigma^f)$ ].

To solve the effective impurity problem, we make use of the hybridization expansion CT-QMC method.<sup>33-35</sup> This method allows us to access the strong interaction region down to low temperatures, which is suitable for the present purpose. In the following,  $D$  is taken as the energy unit.

### III. EFFECTS OF INTERORBITAL CORRELATION

In this section we highlight the effects due to  $U_{ff}$  and  $U_{cf}$  by setting  $U_{cc} = 0$  for a while. It is known that in the ordinary periodic Anderson model with  $U_{cf} = 0$  the paramagnetic Kondo insulating phase and the AF phase compete with each other at half-filling according to the strength of the  $f$ - $f$  interaction: for small (large)  $U_{ff}$ , the AF (Kondo insulating) phase is stabilized at low temperatures. In the presence of  $U_{cf}$ , the CO phase should also appear at low temperatures. Possible spin/orbital configurations for the AF and CO phases are sketched in Fig. 1. We first discuss the competition of the above phases by changing the  $c$ - $f$  hybridization  $V$  and the  $c$ - $f$  interaction  $U_{cf}$  systematically.

The order parameter calculated for the AF phase is plotted in Fig. 2. Note that in the AF and PM phases, the  $f$ -electron filling is equal to unity, so that the system is in the Kondo regime for  $U_{ff} = 3$ . In Fig. 2(a) we can see that as a result

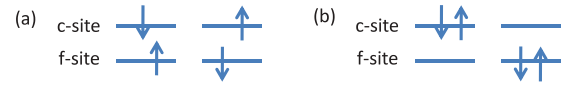


FIG. 1. (Color online) Spin and orbital configurations for (a) AF phase and (b) CO phase.

of the temperature effect, the AF order disappears and the high-temperature PM phase is stabilized in  $V < 0.29$ , which should be distinguished from the Kondo insulating phase discussed below. With increasing hybridization  $V$ , the RKKY interaction becomes dominant and the AF phase emerges via a second-order transition, giving rise to the increase in the AF moments. Further increase in  $V$  again suppresses the antiferromagnetic moments due to the development of the Kondo effect. Therefore, when the hybridization is weak, the system is in the high-temperature PM phase, while for strong hybridization, the system is in the PM phase which is adiabatically connected to the Kondo insulator. In Fig. 2(b) the AF moments are plotted as a function of the  $c$ - $f$  interaction  $U_{cf}$ . In this figure the suppression of the AF moments by the  $c$ - $f$  correlations is indeed observed, which is attributed to the enhancement of the Kondo effect. This can be confirmed by noticing that the  $c$ - $f$  exchange interaction is written as  $J_{cf} = 4V^2/(U_{ff} - 2U_{cf})$ . From this estimation we find that the increase in magnitude of the exchange interaction causes the enhancement of the Kondo effect.

Now we turn to the CO phase. If the  $c$ - $f$  hybridization is weak, the system is expected to be in the AF ordered phase at low temperatures, which should be changed into the CO phase in the presence of strong  $c$ - $f$  correlations. The order parameter for the CO phase at  $V = 0.036$  is plotted in Fig. 3(a). In this figure a discontinuous change in the order parameter accompanied by a hysteresis is observed. Namely, the CO transition at  $V = 0.036$  is of first order. On the other hand, as seen in Fig. 3(b), the transition is changed to second order in the  $V = 0.1$  case. Thus, these behaviors indicate the existence of a critical end point of the first-order transition when we change  $U_{cf}$  or  $V$ .

Performing similar calculations for different choices of parameters, we end up with the rich phase diagram for  $T = 0.02$  and  $U_{ff} = 3$ , as shown in Fig. 4. As mentioned above, in the large  $U_{cf}$  region we have the first-order CO transition. The associated coexistence region is represented

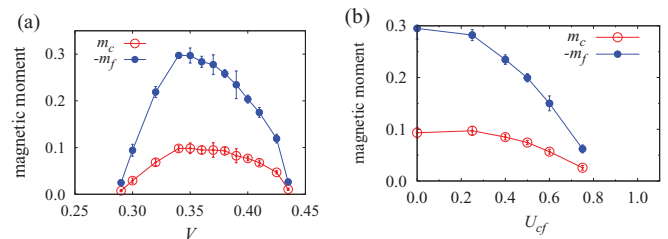


FIG. 2. (Color online) (a) Antiferromagnetic moments as a function of  $V$ :  $T = 0.02$  and  $U_{ff} = 3$ . If the hybridization  $V$  is weak, the AF moments develop with increasing  $V$ , while they decrease in the large  $V$  region. (b) Similar plots as a function of  $U_{cf}$ . The AF moments are suppressed with increasing  $U_{cf}$ . Note that the filling factor of  $f$  electrons is always unity in this calculation.

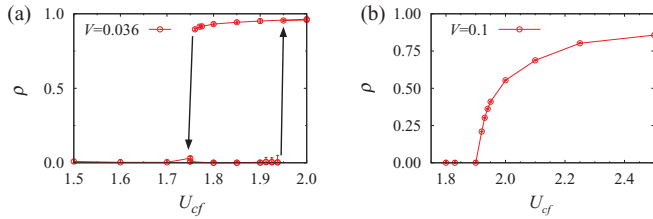


FIG. 3. (Color online) CO parameter plotted against  $U_{cf}$  at  $T = 0.02$ , (a)  $V = 0.036$  and (b)  $0.1$ . At  $V = 0.036$  in (a), the order parameter changes discontinuously and exhibits a hysteresis in  $1.76 < U_{cf} < 1.95$ , while at  $V = 0.1$  in (b), the order parameter changes continuously without any hysteresis.

as a shaded area, where the hysteresis of  $\rho$  is observed. The critical end point is represented by a pink diamond. One notices that the symmetry at the critical end point is unexpectedly high; the CO phase, the AF phase, and the two kinds of PM phases meet each other there. We think that this is somehow accidental. As mentioned above, the PM phase, appearing in the weak  $V$  region, is expected to change into the AF phase at lower temperatures. Since it is not easy to further decrease the temperature due to numerical difficulties, we cannot make a definite statement on this point. However, we will make use of a special trick to decrease the effective temperature in the next section, which indeed demonstrates that the paramagnetic phase in the small  $V$  region should be changed into the AF phase at lower temperatures.

We note that the PM phase realized in the large  $V$  region should be adiabatically connected to the Kondo insulating phase. The corresponding blue line separating the AF phase and the PM phase shifts to the weak  $V$  region with increasing  $U_{cf}$ . This tendency is attributed to the enhancement of the

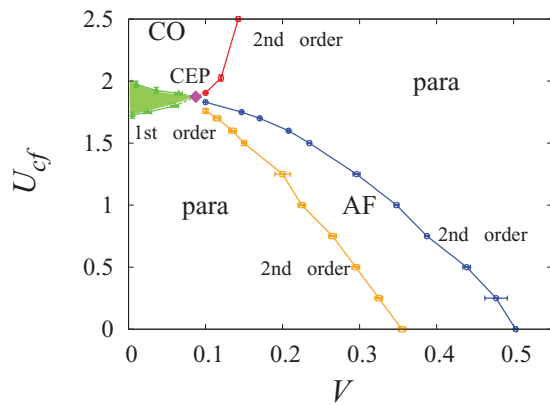


FIG. 4. (Color online) The phase diagram of the extended periodic Anderson model for  $T = 0.02$  and  $U_{ff} = 3$ . The system is in the PM phase in the weak  $V$  region because of the temperature effect. In the strong  $V$  and weak  $U_{cf}$  region the system is in the PM phase, which is smoothly connected to the Kondo insulator. The blue and orange lines separating the AF phase and PM phases represent second-order transitions. In  $V < 0.065$  we can find the first-order transition from the PM phase to the CO phase with increasing  $c$ - $f$  interaction  $U_{cf}$ . In the coexistence region the hysteresis of the CO parameter is observed. For  $V \gtrsim 0.1$  we can find the second-order transition. This fact implies the existence of the critical end point, which is marked with a pink diamond.

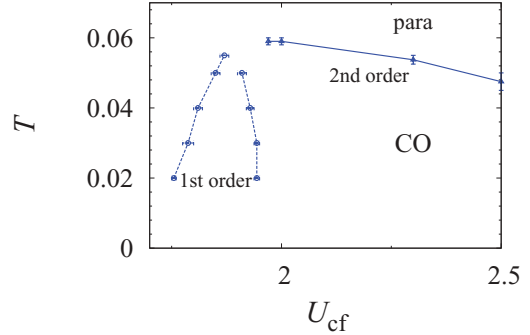


FIG. 5. (Color online) The  $U_{cf}$ - $T$  phase diagram of the extended periodic Anderson model for  $V = 0.036$ ,  $U_{ff} = 3$ . From this figure we can find that the hysteresis region is enlarged with decreasing temperature, implying that the critical point, noted in Fig. 4, remains at zero temperature.

Kondo exchange coupling by the  $c$ - $f$  interaction  $U_{cf}$ , which makes the Kondo insulating state stabler.

Let us now look at the temperature dependence of the CO phase. In Fig. 5 the  $T$ - $U_{cf}$  phase diagram is shown at  $V = 0.036$ . It is seen in this figure that the CO transition changes its character around  $U_{cf} \sim 1.8$ . When  $U_{cf}$  increases, the first-order CO transition suddenly appears at finite temperatures around  $U_{cf} \sim 1.8$ , which is followed by the second-order transition in the large  $U_{cf}$  region where the transition temperature slightly decreases with increasing  $U_{cf}$ . The latter behavior in the transition temperature can be understood in terms of an effective Hamiltonian in the strong  $U_{cf}$  region, which is estimated as  $H_{\text{eff}} = \frac{2t^2}{U_{cf}} \sum_{(i,j),\sigma} (n_{i,\sigma}^c - n_{i,\sigma}^f)(n_{j,\sigma}^c - n_{j,\sigma}^f)$ . Note that the coexistence region is enlarged with decreasing temperature, and is expected to remain at zero temperature. Since the existence of the second-order transition at zero temperature was indicated in our previous results,<sup>29</sup> we would conclude that the critical end point should exist even at zero temperature.

To understand the CO phase in more detail, let us discuss the  $f$ -electron double occupancy and the  $c$ - $f$  spin correlation function. The former is expected to be sensitive to the CO transition. Note that the following results are calculated at  $c$ -electron rich sites. In Fig. 6 the  $f$ -electron double occupancy is plotted as a function of the  $c$ - $f$  hybridization  $V$ . At  $U_{cf} = 1$  without the CO phase, the  $f$ -electron double occupancy smoothly increases with increasing  $V$ . On the other hand, at  $U_{cf} = 2$ , the system is in the CO phase in  $V \lesssim 0.107$ , so that the  $f$ -electron double occupancy rapidly increases around the transition point, and then smoothly decreases with increasing  $V$  in the PM phase. These different behaviors between the  $U_{cf} = 1$  and  $2$  cases are attributed to the difference in the charge configurations of the ground states at  $V = 0$ . Spin and orbital configurations of the ground states for each  $U_{cf}$  case are drawn in Fig. 1. At  $U_{cf} = 1$  the electron density of each orbital is unity, and the increase in  $V$  contributes to the increase in the  $f$ -electron double occupancy. On the other hand, at  $U_{cf} = 2$ , electrons tend to occupy the same orbital to avoid the  $c$ - $f$  interaction. In this situation, with increasing  $V$ , electrons easily hop to the other orbitals.

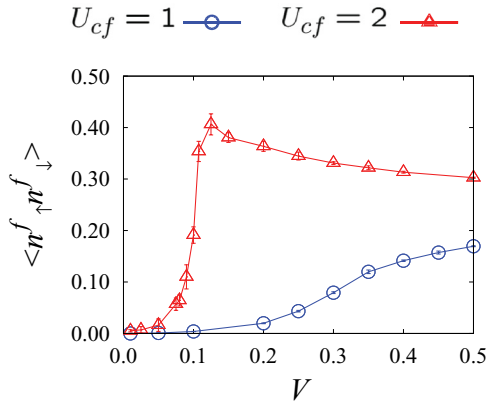


FIG. 6. (Color online) Double occupancy of  $f$  electrons as a function of  $V$  for  $T = 0.02$ ,  $U_{cf} = 1$  and 2. The rapid decrease in  $V < 0.107$  is due to charge ordering for the sublattice where the density of  $f$  electrons is small ( $f$ -electron poor sites).

If hybridization  $V$  is weak, the above tendency becomes more prominent near the CO transition point. In Fig. 7(a) the  $f$ -electron double occupancy is plotted as a function of  $U_{cf}$ . At  $V = 0.1$  the sharp increase in double occupancy is observed, but is smeared for  $V = 0.4$ . This is also the case for the  $c$ - $f$  spin correlation plotted in Fig. 7(b); at  $V = 0.1$  the  $c$ - $f$  spin correlation rapidly increases around  $U_{cf} \sim 1.83$ , which is due to the enhancement of the Kondo effect around the CO transition, but such singular behavior is completely washed out for  $V = 0.4$ .

Finally we show in Fig. 8 the order parameters for each phase and the  $c$ - $f$  spin correlation function at different temperatures. In this figure, at  $T = 0.02$ , the  $c$ - $f$  spin correlation increases near the transition point of the AF phase, which implies that the increase in the  $c$ - $f$  spin correlation reflects the enhancement of the Kondo effect or AF fluctuations. We note, however, that at higher temperatures where the system has no antiferromagnetic order, a similar behavior in the  $c$ - $f$  spin correlation is observed. This naturally leads us to conclude that the peculiar behavior of the  $c$ - $f$  spin correlation indeed originates from the enhancement of the Kondo effect. As is the case for the  $f$ -electron double occupancy, this behavior is smeared with increasing hybridization.

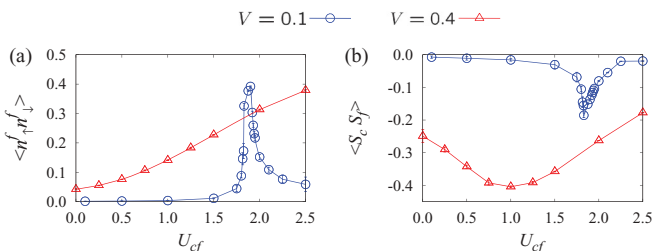


FIG. 7. (Color online) Correlation functions plotted against  $U_{cf}$  at  $T = 0.02$ : (a)  $f$ -electron double occupancy and (b)  $c$ - $f$  electron spin correlation function. In  $1.9 \lesssim U_{cf}$  the system is in the CO phase.

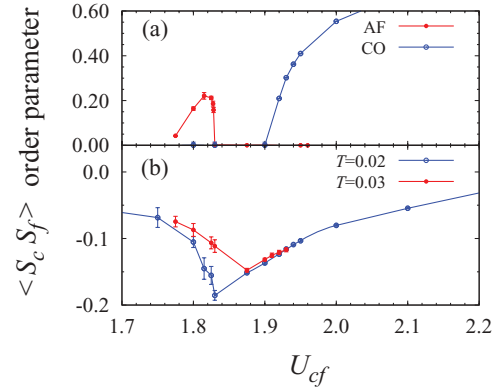


FIG. 8. (Color online) (a) Order parameters of each phase at  $T = 0.02$ ,  $V = 0.1$ . The red (blue) line represents the AF (CO) phase, respectively. (b)  $c$ - $f$  electron correlation at  $V = 0.1$ :  $T = 0.02$  (red line) and  $T = 0.03$  (blue line).

#### IV. EFFECTS OF CONDUCTION ELECTRON CORRELATIONS

We now discuss the effects of Hubbard-type interaction  $U_{cc}$  between  $c$  electrons on the phase diagram. The study of these effects has two important aspects. One point is, of course, that it should clarify the competition between  $U_{ff}$ ,  $U_{fc}$ , and  $U_{cc}$ . The other point is that it will shed light on how the critical point, with seemingly high symmetry found in Fig. 4 at  $U_{cc} = 0$ , should be changed when the temperature is further lowered. Since it is not easy to lower the temperature for the model in Fig. 4 due to some technical problems in numerical calculations, we effectively decrease the temperature by introducing  $U_{cc}$  especially in the AF region.

A prototypical phase diagram obtained for finite  $U_{cc}$  is shown in Fig. 9. Although generic features of the phase diagram are similar to those in Fig. 4 at  $U_{cc} = 0$ , it is seen that the  $c$ -electron correlations substantially affect the properties of the AF phase. We indeed notice that the paramagnetic phase found in the small  $V$  region of Fig. 4 is completely replaced by the AF phase in the presence of  $U_{cc}$ . This is due to the fact that the introduction of  $U_{cc}$  gives rise to the Heisenberg exchange interaction among conduction electrons, stabilizing the AF phase in collaboration with the RKKY interaction between  $f$  electrons. This effectively raises the AF transition temperature,

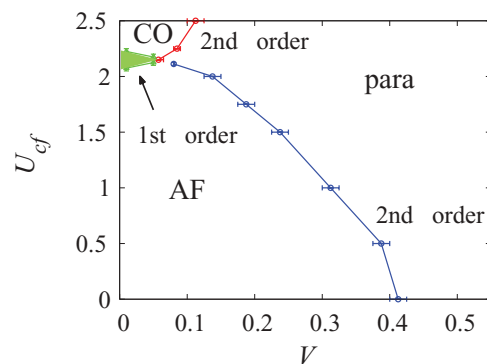


FIG. 9. (Color online) The  $V$ - $U_{cf}$  phase diagram at  $T = 0.02$ ,  $U_{cc} = 1$ . Note that  $c$ -electron correlations slightly suppress the CO phase and extend the AF phase toward the large  $U_{cf}$  region.

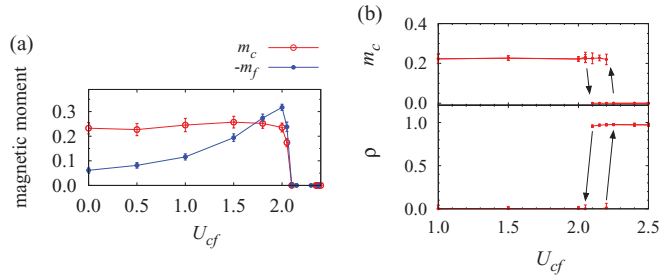


FIG. 10. (Color online) (a) Magnetic moments at  $T = 0.02$ ,  $V = 0.1$ . (b) Order parameters of each phase at  $T = 0.02$ ,  $U_{cc} = 1$ , and  $V = 0.01$ . The magnetic moment at the  $c$  orbital (order parameters of the CO phase) is plotted in the upper (lower) panel. The magnetic moment of the  $f$  orbital is much smaller than that of the  $cb$  orbital.

which exceeds the temperature  $T = 0.02$  employed in Fig. 4. This provides us with some implications about the destiny of the extremely highly symmetric critical point in Fig. 4 where many transition lines merge at the same point. Since we find here that “effectively lowering temperature” completely stabilizes the AF state at  $T = 0.02$  and lifts the accidental high symmetry at the critical point in Fig. 9, we believe that the qualitatively similar phase diagram should be obtained if we can further decrease the temperature in Fig. 4.

Within the AF phase in Fig. 9, we naturally expect a crossover behavior according to the strengths of  $U_{cc}$  and  $U_{cf}$ . Let us focus on the region of weak hybridization (e.g.,  $V = 0.1$ ). For small  $U_{cf}$ , the system has the AF order driven by the Heisenberg interaction between  $c$  electrons originating from  $U_{cc}$ . With increasing  $c$ - $f$  interactions  $U_{cf}$ , as discussed above, the RKKY exchange interaction is gradually enhanced and becomes dominant to stabilize the AF phase. This can be indeed seen in Fig. 10(a), where the magnetic moments are plotted as a function of the  $c$ - $f$  interaction; for the small  $U_{cf}$  region, the magnetization of conduction electrons  $m_c$  induced via the Heisenberg interaction is dominant, while for larger  $U_{cf}$ ,  $m_f$  induced via the RKKY exchange interaction becomes dominant especially around  $U_{cf} \sim 1.8$ . These two regions in the AF phase are adiabatically connected via a crossover.

In contrast to the AF phase, the essential features in the CO phase seem to be little affected by  $U_{cc}$ , as seen in Fig. 9 in comparison with Fig. 4. This implies that the CO phase should be robust, as far as the system is in the region of large  $U_{cf}$  and small  $V$ . Note that the critical value for the CO transition is slightly increased by  $U_{cc}$  since the AF state becomes stabler in the presence of  $U_{cc}$  (the paramagnetic phase at  $U_{cc} = 0$  is indeed changed to the AF phase). The order parameters for CO and AF are shown in Fig. 10(b), where we can clearly see the hysteresis behavior signaling the first-order transition. Similarly, we have observed qualitatively the same behaviors in the  $f$ -electron double occupancy and the  $c$ - $f$  electron correlations, as discussed in the previous section. We can thus

say that the effects of  $U_{cc}$  mainly modify the characteristics of the AF magnetic phase, but give a minor change to the CO properties.

## V. SUMMARY AND DISCUSSION

In this paper we have studied the  $c$ - $f$  correlation effects on heavy fermion systems with special focus on the emergence of the CO phase. Employing the DMFT and continuous time-quantum Monte Carlo simulations, it has been clarified how the AF phase, observed in the ordinary periodic Anderson model, changes into the CO phase in the strong  $c$ - $f$  correlation region. With increasing  $c$ - $f$  electron interaction, the inter-orbital interaction first increases the magnetic moment. Further increase in the interaction strength enhances the Kondo effect, which in turn suppresses the AF phase and stabilizes the CO phase. Near the CO transition, a sharp increase of  $c$ - $f$  singlet correlation is observed. This behavior is considered to reflect the enhancement of the Kondo effect. With the systematic analysis in the plane of hybridization vs  $c$ - $f$  interaction, the existence of the critical end point of the first-order CO transition has also been observed.

Regarding the effects due to the  $c$ - $f$  interaction, the VT is also important, so that some comments are in order for the VT here. It is known that the  $c$ - $f$  correlation possibly induces the VT, but in our analysis the VT has not been observed. This is because we have restricted ourselves to the particle-hole symmetric case. To discuss the possibility of the VT, it is necessary to study the system with strong valence fluctuations away from the symmetric case. It is interesting to discuss the competition between the AF, VT, and CO transitions by properly tuning the valence fluctuations.

Further studies on the relation between the present CO phase and that observed for  $\text{Eu}_3\text{S}_4$  should be interesting. As mentioned in the Introduction, in these compounds a CO phase is observed with decreasing temperature, where the valence of rare-earth elements is spatially modulated and local spins remain even in the CO phase, which lead to the magnetic order in the lower temperature region.<sup>36,37</sup> Our analysis here may not be straightforwardly applied to the experiment. To clarify this point, it remains an interesting issue to study the possibility of CO phase with local spin degrees of freedom.

## ACKNOWLEDGMENTS

We acknowledge fruitful discussions with T. Ohashi. A part of numerical computations was done at the Supercomputer Center at ISSP, University of Tokyo, and also at YITP, Kyoto University. This work was supported by KAKENHI (No. 21740232, No. 20104010), and the Grant-in-Aid for the Global COE Programs, The Next Generation of Physics, Spun from Universality, and Emergence from MEXT of Japan. N.K. is supported by JSPS through the “Funding Program for World-Leading Innovative R&D on Science and Technology” (FIRST Program).

<sup>1</sup>F. Steglich, J. Aarts, C. D. Bredl, W. Lieke, D. Meschede, W. Franz, and H. Schafer, *Phys. Rev. Lett.* **43**, 1892 (1979).

<sup>2</sup>D. Jaccard, H. Wilhelm, K. Almani-Yadri, and E. Vargoz, *Physica B* **259–261**, 1 (1999).

- <sup>3</sup>A. T. Holmes, D. Jaccard, and K. Miyake, *Phys. Rev. B* **69**, 024508 (2004).
- <sup>4</sup>H. Q. Yuan, F. M. Grosche, M. Deppe, C. Geibel, G. Sparn, and F. Steglich, *Science* **302**, 2104 (2003).
- <sup>5</sup>H. Q. Yuan, F. M. Grosche, M. Deppe, G. Sparn, C. Geibel, and F. Steglich, *Phys. Rev. Lett.* **96**, 047008 (2006).
- <sup>6</sup>K. Miyake, O. Narikiyo, and Y. Onishi, *Physica B* **259–261**, 676 (1999).
- <sup>7</sup>Y. Onishi and Y. Miyake, *J. Phys. Soc. Jpn.* **69**, 3955 (2000).
- <sup>8</sup>S. Watanabe, M. Imada, and K. Miyake, *J. Phys. Soc. Jpn.* **75**, 043710 (2006).
- <sup>9</sup>Y. Saiga, T. Sugibayashi, and D. S. Hirashima, *J. Phys. Soc. Jpn.* **77**, 114710 (2008).
- <sup>10</sup>S. Suga, A. Sekiyama, S. Imada, J. Yamaguchi, A. Shigemoto, A. Irizawa, and K. Yoshimura, *J. Phys. Soc. Jpn.* **78**, 074704 (2009).
- <sup>11</sup>I. Felner, I. Nowik, D. Vaknin, U. Potzel, J. Moser, G. M. Kalvius, G. Wortmann, G. Schmiester, G. Hilscher, E. Gratz, C. Schmitzer, N. Pillmayr, K. G. Prasad, H. de Waard, and H. Pinto, *Phys. Rev. B* **35**, 6956 (1987).
- <sup>12</sup>K. Yoshimura, T. Nitta, M. Mekata, T. Shimizu, T. Sakakibara, T. Goto, and G. Kido, *Phys. Rev. Lett.* **60**, 851 (1988).
- <sup>13</sup>J. K. Freericks and V. Zlatic, *Phys. Rev. B* **58**, 322 (1998).
- <sup>14</sup>S. Watanabe, A. Tsuruta, K. Miyake, and J. Flouquet, *Phys. Rev. Lett.* **100**, 023401 (2008).
- <sup>15</sup>A. C. Hewson and P. S. Riseborough, *Solid State Commun.* **22**, 379 (1977).
- <sup>16</sup>A. V. Goltsev and G. Bruls, *Phys. Rev. B* **63**, 155109 (2001).
- <sup>17</sup>A. Hübsch and K. W. Becker, *Eur. Phys. J. B* **52**, 345 (2006).
- <sup>18</sup>T. Sugibayashi and D. S. Hirashima, *J. Phys. Soc. Jpn. Suppl.* **75**, 244 (2006).
- <sup>19</sup>A. K. Zhuravlev, V. Yu. Irkhin, and M. I. Katsnelson, *Eur. Phys. J. B* **55**, 377 (2007).
- <sup>20</sup>L. Craco, *Phys. Rev. B* **77**, 125122 (2008).
- <sup>21</sup>V.-N. Phan, A. Mai, and K. W. Becker, *Phys. Rev. B* **82**, 045101 (2010).
- <sup>22</sup>S. Watanabe and K. Miyake, *Phys. Rev. Lett.* **105**, 186403 (2010).
- <sup>23</sup>K. Kubo, *J. Phys. Soc. Jpn.* **80**, 114711 (2011).
- <sup>24</sup>H. Ohara, S. Sakai, Y. Konoike, T. Toyoda, K. Yamawaki, and M. Tanaka, *Physica B* **350**, 353 (2004).
- <sup>25</sup>A. Ochiai, T. Suzuki, and T. Kasuya, *J. Phys. Soc. Jpn.* **59**, 4129 (1990).
- <sup>26</sup>T. Sugibayashi, Y. Saiga, and D. S. Hirashima, *J. Phys. Soc. Jpn.* **77**, 024716 (2008).
- <sup>27</sup>Y. Dubi and A. V. Balatsky, *Phys. Rev. Lett.* **106**, 086401 (2011).
- <sup>28</sup>J. J. Su, Y. Dubi, P. Wölfle, and A. V. Balatsky, [arXiv:1010.0767](https://arxiv.org/abs/1010.0767).
- <sup>29</sup>T. Yoshida, T. Ohashi, and N. Kawakami, *J. Phys. Soc. Jpn.* **80**, 064710 (2011).
- <sup>30</sup>W. Metzner and D. Vollhardt, *Phys. Rev. Lett.* **62**, 324 (1989).
- <sup>31</sup>E. M. Hartmann, *Z. Phys. B* **74**, 507 (1989).
- <sup>32</sup>A. Georges, G. Kotliar, W. Krauth, and M. J. Rozenberg, *Rev. Mod. Phys.* **68**, 13 (1996).
- <sup>33</sup>P. Werner, A. Comanac, L. de'Medici, M. Troyer and A. J. Millis, *Phys. Rev. Lett.* **97**, 076405 (2006).
- <sup>34</sup>P. Werner and A. J. Millis, *Phys. Rev. B* **74**, 155107 (2006).
- <sup>35</sup>K. Haule, *Phys. Rev. B* **75**, 155113 (2007).
- <sup>36</sup>E. Gorlich, H. U. Hryniewicz, R. Kmieć, K. Latka, and K. Tomala, *Phys. Status Solidi B* **64**, K147 (1974).
- <sup>37</sup>V. N. Antonov, B. N. Harmon, and A. N. Yaresko, *Phys. Rev. B* **72**, 085119 (2005).